Cell Stress and Chaperones (2010) 15:415–421
DOI 10.1007/s12192-009-0157-2

ORIGINAL PAPER

Domain *a'* of protein disulfide isomerase plays key role in inhibiting α-synuclein fibril formation

Han Cheng · Lei Wang · Chih-chen Wang

Received: 20 September 2009 / Revised: 30 October 2009 / Accepted: 2 November 2009 / Published online: 4 December 2009

Abstract α-Synuclein (αSyn) is the main component of Lewy bodies formed in midbrain dopaminergic neurons which is a pathological characteristic of Parkinson's disease. It has been recently showed to induce endoplasmic reticulum (ER) stress and impair ER functions. However, the mechanism of how ER responds to αSyn toxicity is poorly understood. In the present study, we found that protein disulfide isomerase (PDI), a stress protein abundant in ER, effectively inhibits αSyn fibril formation in vitro. In PDI molecule with a structure of *abb'xa'c*, domain *a'* was found to be essential and sufficient for PDI to inhibit αSyn fibril formation. PDI was further found to be more avid for binding with intermediate species formed during αSyn fibril formation, and the binding was more intensive in the later lag phase. Our results provide new insight into the role of PDI in protecting ER from the deleterious effects of misfolded protein accumulation in many neurodegenerative diseases.

Keywords Protein disulfide isomerase · α-Synuclein · Fibril · Isothermal titration calorimetry

Introduction

Parkinson's disease (PD), the second most common neurodegenerative disease, has two prominent pathological characteristics: progressive dopaminergic neuronal loss and the presence of Lewy bodies which consist mainly of α-Synuclein (αSyn); (Polymeropoulos et al. 1997; Spillantini et al. 1998). Some cases of early familial PD were identified as being linked to three αSyn mutations, namely A53T, A30P, and E46K (Kruger et al. 1998; Munoz et al. 1997; Zarranz et al. 2004), these mutations accelerate the fibrillation or oligomerization of the mutated proteins in vitro (Conway et al. 2000). Overexpression of αSyn in flies (Feany and Bender 2000), mice (Masliah et al. 2000), and primates (Kirik et al. 2003) is sufficient to trigger PD, suggesting the important roles αSyn fibrillation plays in the disease pathogenesis.

αSyn, initially identified as a synaptic vesicle-associated protein, is also found in the cytosol and nucleus (Kontopoulos et al. 2006; Lee et al. 2005). In immunogold electron microscopy examination of rat brain neurons, the αSyn concentration was found to be higher in endoplasmic reticulum (ER) than in cytoplasmic region (Zhang et al. 2008). Synthesized αSyn in yeast was found to be translocated from the ER to the Golgi and further to the plasma membrane through a classical secretion pathway (Dixon et al. 2005). Recently, αSyn has been reported to be involved in the impairment of ER functions. Overexpression of αSyn A53T mutant in differentiated PC12 cells induces ER stress (Smith et al. 2005), and overexpression of wild-type αSyn or the A53T mutant in yeast induces unfolded protein response and blocks ER-Golgi trafficking (Cooper et al. 2006; Gitler et al. 2008).

Protein disulfide isomerase (PDI) is a multifunctional stress protein abundant in ER with both isomerase and chaperone activities (Yao et al. 1997). It facilitates the folding, unfolding, and translocation of many proteins (Ellgaard and Ruddock 2005; Papp et al. 2003) and protects ER from damage. PDI is an essential protein, and is

H. Cheng · L. Wang · C.-c. Wang (✉)
National Laboratory of Biomacromolecules,
Institute of Biophysics, Chinese Academy of Sciences,
Beijing 100101, China
e-mail: chihwang@sun5.ibp.ac.cn

H. Cheng
Graduate School of the Chinese Academy of Sciences,
Beijing 100049, China

expressed in nearly all tissues, including neural tissue and various cultured neural cell lines (www.proteinatlas.org). PDI can prevent neurotoxicity associated with ER stress and protein misfolding, whereas S-nitrosylation of PDI suppresses this protective effect in PD or Alzheimer's disease (Uehara et al. 2006). However, the interactions of PDI and αSyn have not yet been reported so far to the best of our knowledge.

In our experiments, we examined how PDI affected αSyn fibril formation and found out for the first time that PDI can effectively inhibit αSyn fibril formation in vitro, very likely via interacting with αSyn intermediates formed during the course. And we also identified the *a'* domain of PDI as crucial to PDI's ability of inhibiting αSyn fibril formation.

Materials and methods

Protein expression and purification

The PCR products of the *a* and *a'c* fragments amplified from pQE30-PDI were ligated into pQE30 with *Bam*HI/*Hind*III sites to construct corresponding expression plasmids. The coding sequence of DsbCn-*a'*c was constructed by overlapping PCR products amplified from pQE30-PDI and pQE60-DsbC, respectively, and the gene fusion digested with *Bam*HI/*Hind*III was then ligated into pQE30. Full-length human PDI, PDI fragments (PDI (1–462), *abb'x*, *bb'xa'*, *a*, and *a'c*), DsbC, and DsbCn-*a'c* were expressed in *Escherichia coli* M15 [REP4] with a N-terminal His tag (MRGSHHHHHHGS) and purified by using a nickel-nitrilotriacetic acid column as described previously (Wang et al. 2009). Recombinant human αSyn was expressed in BL21 (DE3) and was purified by chromatography of the supernatant after osmotic shock on a Q-Sepharose fast-flow column as described previously (Huang et al. 2005). Concentration of αSyn was determined spectrophotometrically by using the absorption coefficient $A_{280}^{0.1\%}$ of 0.354 or by the bicinchoninic acid method with bovine serum albumin (BSA) as a standard. The concentrations of PDI and domain combinations were determined by Bradford assay with BSA as a standard.

Determination of αSyn fibril formation by Thioflavin T fluorescence

The kinetics of fibril formation of αSyn was monitored using Thioflavin T (ThT) binding fluorescence as described (Huang et al. 2006). Briefly, αSyn solution at 70 μM in buffer A (50 mM Tris–HCl, 0.2 M NaCl, 0.05% NaN_3 (*w*/*v*), pH 8.0) with or without different concentrations of PDI proteins were incubated with shaking at 37°C. An aliquot of 8-μl reaction mixture was taken at time intervals for ThT fluorescence measurement.

Electron microscopy

A 5-μl aliquot was taken from the aggregation reaction mixture at 48 h of fibril formation, adsorbed onto a glow-discharged carbon support film, washed twice using 20 μl distilled water, and negatively stained with 2% (*w*/*v*) uranyl acetate. Micrographs were recorded on Gatan Digital Micrograph at ×14,500 magnification on a Philp Tecnai 20 electron microscope.

Protein interaction characterization by gel filtration

Prefibrillar αSyn was prepared as described by Volles et al. (Volles et al. 2001) i.e. a concentrated αSyn solution at ~1-2 mM in buffer B (buffer A supplemented with 10 mM 2-mercaptoethanol) was eluted on a Superdex 200 10/300 GL column (Amershan Phamacia Biotech) at 0.5 ml/min, and the protein in the void peak was collected as prefibrillar αSyn. An 800 μl solution of 5 μM prefibrillar αSyn (monomer concentration) or 10 μM αSyn in buffer B was incubated with or without 10 μM PDI proteins at room temperature for 2 h and eluted on the same column, and the elution peaks were collected, precipitated by acetone at -20°C, and analyzed by 15% SDS-PAGE.

Isothermal titration calorimetry measurement

Thermodynamic parameters associated with interactions between PDI proteins and αSyn were measured on a VP-isothermal titration calorimetry (ITC) titration calorimeter (MicroCal, Inc.) at 25°C. At 0, 3, 6, and 48 h of αSyn fibril formation, reaction samples were taken and diluted to 30 μM (αSyn monomer concentration) and loaded into the sample cell, and a solution of 300 μM PDI proteins was placed in the injection syringe. The first injection of 5 μl was followed by 29 injections of 10 μl. The PDI proteins were injected into buffer alone, and the dilution heats were measured and subtracted from the experiment data prior to data analysis. Data were analyzed using MicroCal ORIGIN software supplied with the instrument. All experiments were performed in buffer C (25 mM Tris–HCl, 0.1 M NaCl, 0.05% NaN_3 (*w*/*v*), pH 8.0). The stirring rate was 300 rpm.

Statistics

Data were expressed as mean ± standard deviation (SD). Differences among means were analyzed by using unpaired one-tailed or two-tailed *t* test. A *p* value of 0.05 or less was judged to be significant.

Results

PDI suppresses αSyn fibril formation

Under the established conditions, the αSyn fibril formation monitored by using ThT fluorescence in 1–2 days showed a sigmoid growth curve, which included an initial lag phase, a subsequent exponential growth phase, and a final equilibrium phase (Fig. 1a). When the molar ratio of PDI to αSyn was 0.1, the increase in ThT fluorescence observed in the absence of PDI was inhibited by ~75%, and PDI with higher molar ratios against αSyn, e.g., 0.2 and 0.5, showed only little further effects (Fig. 1b). PDI itself showed little ThT fluorescence over the experiment course (Fig. 1a). BSA, a protein with no chaperone activity but a molecular weight similar to that of PDI, was used as a negative control because it did not inhibit αSyn fibril formation (Fig. 1a). Yeast prion protein Ure2p also forms fibril in vitro, and this process was reportedly inhibited by Ssa1p (Savistchenko et al. 2008), the yeast homolog of human Hsp70, another potent inhibitor of αSyn fibril formation (Dedmon et al. 2005; Huang et al. 2006). However, we observed that PDI, unlike Hsp70, did not inhibit the fibril formation of Ure2p (data not shown), suggesting that PDI interacts with αSyn specifically to inhibit its fibril formation.

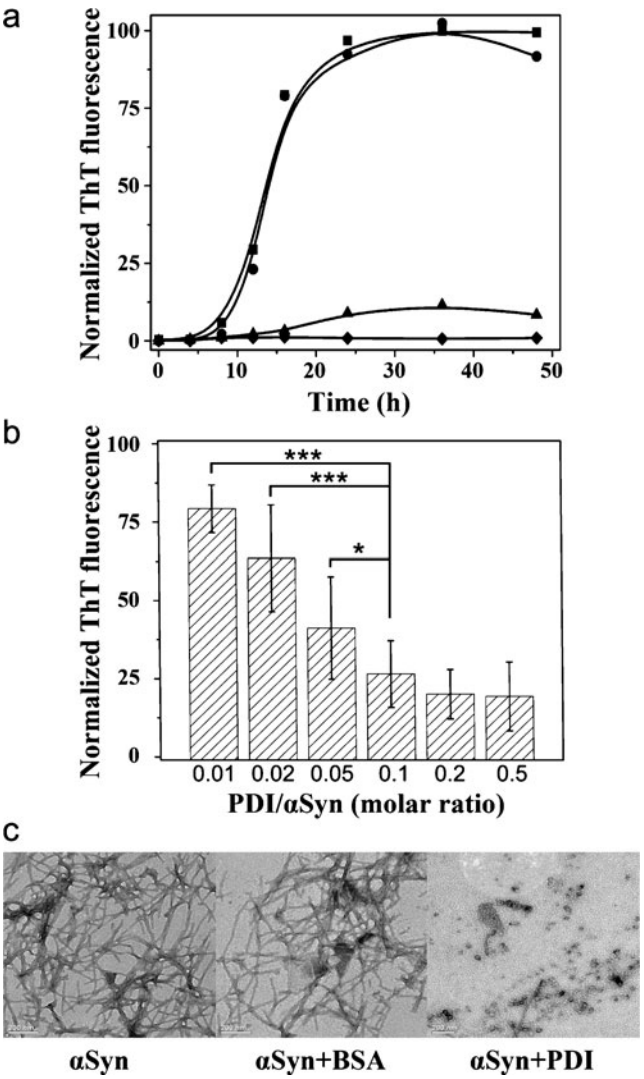

Fig. 1 Inhibition of αSyn fibril formation by PDI. **a** The experiments of fibril formation of 70 μM αSyn in the absence (*filled square*)/ presence of 35 μM PDI (*filled triangle*) or BSA (*filled circle*) and fibril formation of PDI alone (*filled diamond*) were carried out as described in the text, and ThT fluorescence at 482 nm were measured at different time points as indicated and normalized. **b** Fibril formation of 70 μM αSyn in the presence of PDI at various molar ratios were assessed with respect to ThT fluorescence at 48 h. Data are expressed as mean ± SD (*$p<0.05$, ***$p<0.001$ by unpaired one-tailed *t* test ($n\geq4$)). **c** Electron micrographs of 70 μM αSyn fibril formation at 48 h in the equilibrium phase in the absence and presence of 35 μM PDI or BSA. *Scale bar* 200 nm

Figure 1c shows the electron microscopy images of the morphology of αSyn aggregates formed at the equilibrium phase. When αSyn was incubated alone, it formed long tangled fibrils which were micrometers long and ~10 nm in diameter. In the presence of PDI there were only amorphous αSyn aggregates instead of fibrils. In the presence of BSA, αSyn still formed long tangled fibrils.

Effects of PDI domains on αSyn fibril formation

PDI comprises four thioredoxin (Trx) domains: two catalytic domains, *a* and *a'*, separated by two non-catalytic domains, *b* and *b'*, followed by a C-terminal region *c*. In addition, there is a short linker region "*x*" situated between the *b'* and *a'* domains. The *b'* domain of PDI has been identified as the primary site for binding short peptides to PDI and essential for binding more complex substrates to PDI while the *a* and *a'* domains of PDI contribute to binding large substrates to PDI (Klappa et al. 1998; Pirneskoski et al. 2004).

For the purpose of locating the part of PDI molecule which is responsible for its ability of inhibiting αSyn fibril formation, we constructed several PDI domain combinations (Fig. 2a). As shown in Fig. 2b and c, PDI (1–462), i.e., the PDI with the *c* region removed, inhibited αSyn fibril formation to a similar extent as full-length PDI did, indicating that the *c* region of PDI is not required in inhibiting αSyn fibril formation. The *abb'x* fragment, with both domain *a'* and *c* region removed from full-length PDI, showed much weaker inhibiting effect, i.e., it inhibited only ~40% of αSyn fibril formation; while the *bb'xa'* fragment containing domain *a'* inhibited αSyn fibril formation to the same extent as full-length PDI did. This suggests that domain *a'* is required for inhibiting αSyn fibril formation. We further examined the inhibiting ability of fragment *a'c* (which was used instead of domain *a'* alone because of its

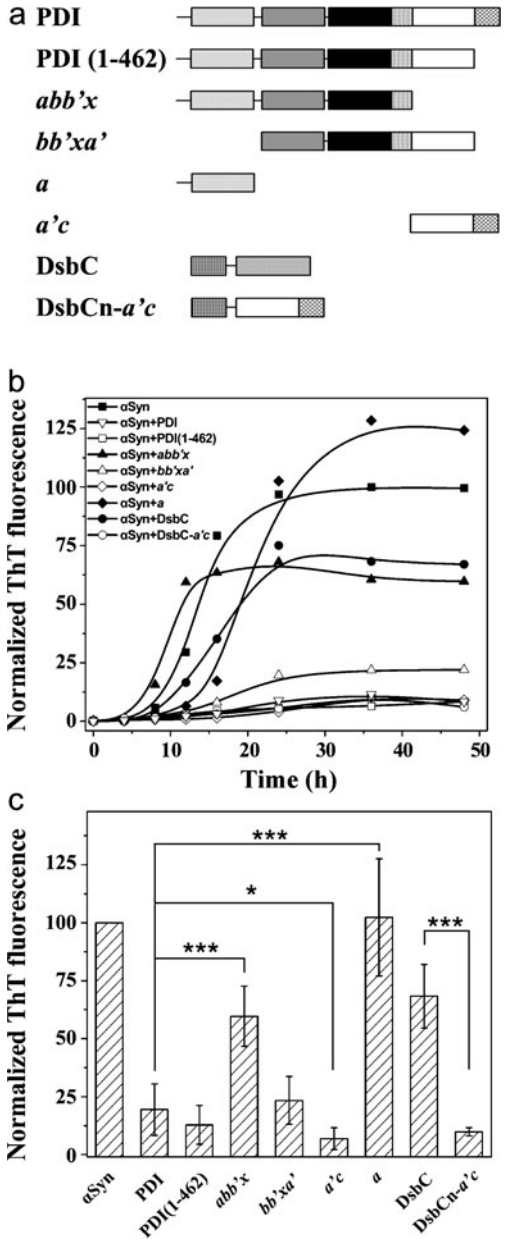

Fig. 2 Inhibition of αSyn fibril formation by PDI domains. **a** Schematic representation of domain structure of PDI molecule and domain combinations. **b** Fibril formation of 70 μM αSyn in the absence (*filled square*) and presence of 35 μM PDI (*unfilled inverted triangle*), PDI (1–462; *unfilled square*), *abb'x* (*filled triangle*), *bb'xa'* (*unfilled triangle*), *a* (*filled diamond*), *a'c* (*unfilled diamond*), DsbC (*filled circle*), and DsbCn-*a'c* (*unfilled circle*) were measured at various time points (**b**) or at 48 h (**c**) as indicated by using ThT fluorescence at 482 nm and the measured data were normalized. The data in **c** were expressed as mean ± SD (*p<0.05, ***p<0.001 by unpaired one-tailed t test (n≥4))

much better solubility and the *c* region being negligible in inhibiting αSyn fibril formation). It was observed that fragment *a'c* alone did inhibit αSyn fibril formation as effectively as full-length PDI did. Although domains *a* and *a'* share 36.8% identity with each other, domain *a* showed no effect on αSyn fibril formation. We further designed a domain chimera DsbCn-*a'c* by replacing the C-terminal Trx domain of *E. coli* DsbC with domain *a'c* of PDI to further examine the effect of *a'c*. DsbC locates in the periplasm of prokaryotic cells, and is a prokaryotic counterpart of PDI in the ER of eukaryotic cells, but shows no (Huang et al. 2006) or weak inhibiting effect on αSyn fibril formation (Fig. 2b and c). DsbC is a homodimeric protein, and each subunit consists of a C-terminal Trx domain and an N-terminal domain for dimerization. Just as we anticipated, the chimera DsbCn-*a'c*, compared to wild-type DsbC, was much more efficient in inhibiting αSyn fibril formation (p< 0.001; Fig. 2b and c). All the above data provide strong evidence that domain *a'* plays a key role in inhibiting αSyn fibril formation.

Interactions of PDI with intermediate species formed during αSyn fibril formation

The PDI's ability to inhibit αSyn fibril formation indicates the interactions between PDI and αSyn or αSyn intermediate species formed during fibril formation. Firstly we used gel filtration to probe the interaction complexes of PDI and various αSyn species. The incubated mixture of native αSyn and PDI showed only two elution peaks, the positions of which were identical with those of the elution peaks of separately incubated αSyn and PDI, indicating that there is no interaction between αSyn and PDI (data not shown). Artificial prefibrillar αSyn, which was prepared to mimic the intermediate species of αSyn formed in the lag phase, was eluted at a void volume of about 8 ml in a broad peak well separated from the peaks of monomeric αSyn at 13.9 ml and PDI at 12.9 ml. Compared with the prefibrillar αSyn incubated alone, the incubated mixture of PDI and prefibrillar αSyn showed a slightly enlarged void peak (Fig. 3a). SDS-PAGE analysis of the collected void peak showed not only the αSyn band with an apparent molecular mass of 18 kDa but also a band of 57 kDa for PDI (Fig. 3b), indicating the interaction and complex formation between PDI and prefibrillar αSyn. The void peak area of the incubated prefibrillar αSyn with *abb'x* remained unchanged, but that of the incubated prefibrillar αSyn with *bb'xa'* (Fig. 3a) grew larger. The SDS-PAGE analysis of corresponding void volume collections also showed prefibrillar αSyn binding with *bb'xa'* but not *abb'x* (Fig. 3b). The above results showed that PDI interacted with prefibrillar αSyn but not native αSyn, and that *bb'xa'*, *not abb'x*, interacted with prefibrillar αSyn, indicating that the *a'* domain is responsible for the interactions between PDI and prefibrillar αSyn.

ITC can directly detect the heat changes during protein–protein interaction, and the analysis of the reaction heat as a

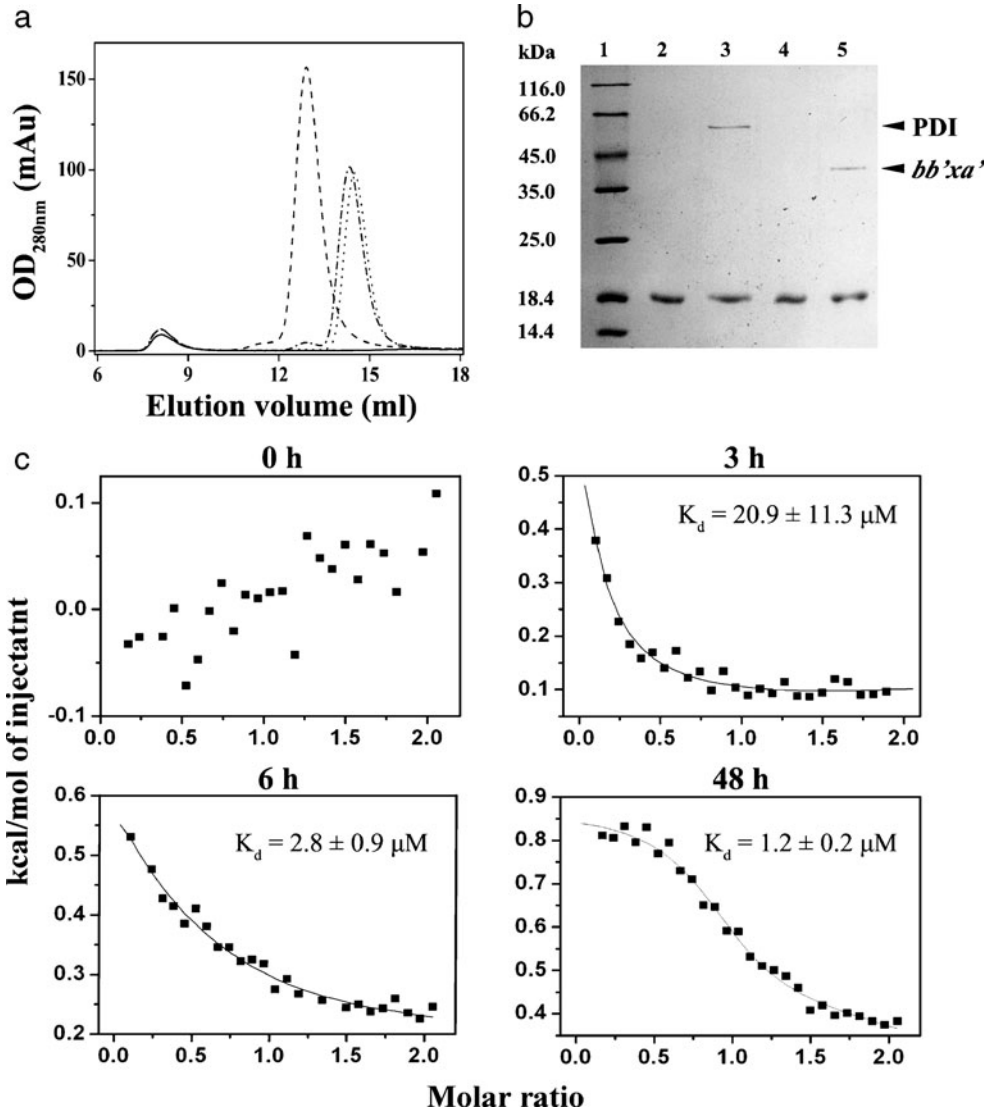

Fig. 3 Interactions between PDI or its domain combinations and αSyn intermediates. **a** Chromatography profiles of incubations of prefibrillar αSyn without (*solid*) and with PDI (*dashed*), *abb'x* (*dotted*), or *bb'xa'* (*dash-dotted*) on a Superdex 200 10/300 GL column. **b** SDS-15%PAGE of void fractions in (**a**). *Lane 1* molecular mass markers, *lane 2* prefibrillar αSyn, *lanes 3–5* co-incubation of prefibrillar αSyn and PDI, *abb'x*, or *bb'xa'*, respectively. **c** ITC data of binding of the PDI proteins to αSyn at 25°C: *squares* represent the integrated binding isotherm at each injection after dilution heat effect correction and molar concentration based normalization, *solid lines* represent the non-linear least squares fit to a three sequential binding sites model, and the best fit parameters of dissociation constant K_d for the first binding event are indicated therein

function of protein concentration provides complete characterization of the thermodynamic properties of protein–protein interactions (Velazquez-Campoy et al. 2004). Thus, ITC was adopted to measure the extent of the interactions between PDI and αSyn in this study. The calorimetric data of the interaction between PDI and 0 h αSyn sample were too small to be fitted into any binding model, indicating no specific binding affinity of PDI to αSyn monomer. The integrated binding isotherms of the samples at 3 and 6 h in the lag phase and at 48 h in the final equilibrium phase fitted a three sequential binding sites model best (Fig. 3c). Since the second and the third binding events might reflect nonspecific weak interactions corresponding to a multi-site low affinity binding of substrates to PDI (Gruber et al. 2006), we only used the first binding parameters for comparison. The interaction between PDI and αSyn intermediate species formed at 3 h was weak with a dissociation constant of 20.9 μM, and the interaction between PDI and αSyn intermediate species formed at 6 h increased significantly with a dissociation constant of 2.8 μM, suggesting PDI was more avid for binding with the intermediate species in the later lag phase. PDI was also observed to be bound with fibril formed at 48 h with a dissociation constant of 1.2 μM. To sum up, the above results indicate that PDI preferentially binds with αSyn intermediate species since the early stages of the assembly, inhibiting the progress of fibril formation.

Discussion

The major findings of this study are that PDI is able to inhibit αSyn fibril formation and domain *a'* of PDI plays a key role in this process. This suggests that the role of domain *a'* in the interactions between PDI and misfolded proteins has been underestimated. Our study also showed that PDI binds with intermediate species in the αSyn fibril formation process to inhibit the fibril formation.

αSyn has recently been shown to be implicated in ER impairment and ER stress (Wang and Takahashi 2007), however, the mechanism remains unknown. It was found that αSyn is more concentrated in ER than in cytoplasmic region (Zhang et al. 2008). Our data provide direct evidence for the interactions between αSyn and PDI, and suggest that PDI, a key component of the protein quality control system in the ER, may counteract the toxicity of αSyn in the ER by binding oligomeric αSyn formed in the early stage and finally inhibiting fibril formation.

PDI can also function in non-ER locations including the cell surface, the extracellular space, the cytosol, and the nucleus (Turano et al. 2002). PDI was shown to co-localize with cytoplasmic aggregates formed by Cu/Zn-superoxide dismutase or its mutants in animal and cell model of familial amyotrophic lateral sclerosis (Atkin et al. 2006). Co-expression of PDI with synphilin-1 in cultured SH-SY5Y cells greatly decreased discrete Lewy-body-like inclusions formed by synphilin-1 in the cytoplasm; and S-nitrosylation of PDI by nitric oxide attenuated this inhibiting effect (Uehara et al. 2006). Moreover, by means of immunohistochemistry, pancreatic PDI was shown to co-localize with αSyn in Lewy bodies in the postmortem human brain tissue from patients with Dementia with Lewy bodies (Conn et al. 2004). Hence, PDI may function in the cytoplasm to play protective roles against αSyn cytotoxicity.

Our study on the interaction between αSyn and PDI suggests a new cellular defense mechanism against αSyn toxicity and a new path in developing therapies against neurodegenerative diseases associated with abnormal protein accumulation. Further studies are required to examine this defense mechanism in detail on the cell and animal level.

Acknowledgements This work was supported by grants from Chinese Ministry of Science and Technology (2006CB806508 and 2006CB910903) and Chinese Academy of Sciences (KSCX2-YW-R-119). We sincerely thank Prof. Hongyu Hu for his generous gift of the plasmid of pET-3a containing human αSyn cDNA and Prof. Sarah Perrett of this Institute for her kind gift of Ure2p protein. Prof. Yigong Shi in Tsinghua University and Prof. Yi Liang in Wuhan University are appreciated for their kind help on ITC experiments.

References

Atkin JD, Farg MA, Turner BJ, Tomas D, Lysaght JA, Nunan J, Rembach A, Nagley P, Beart PM, Cheema SS et al (2006) Induction of the unfolded protein response in familial amyotrophic lateral sclerosis and association of protein-disulfide isomerase with superoxide dismutase 1. J Biol Chem 281:30152–30165

Conn KJ, Gao W, McKee A, Lan MS, Ullman MD, Eisenhauer PB, Fine RE, Wells JM (2004) Identification of the protein disulfide isomerase family member PDIp in experimental Parkinson's disease and Lewy body pathology. Brain Res 1022:164–172

Conway KA, Lee SJ, Rochet JC, Ding TT, Williamson RE, Lansbury PT Jr (2000) Acceleration of oligomerization, not fibrillization, is a shared property of both alpha-synuclein mutations linked to early-onset Parkinson's disease: implications for pathogenesis and therapy. Proc Natl Acad Sci USA 97:571–576

Cooper AA, Gitler AD, Cashikar A, Haynes CM, Hill KJ, Bhullar B, Liu K, Xu K, Strathearn KE, Liu F et al (2006) Alpha-synuclein blocks ER-Golgi traffic and Rab1 rescues neuron loss in Parkinson's models. Science 313:324–328

Dedmon MM, Christodoulou J, Wilson MR, Dobson CM (2005) Heat shock protein 70 inhibits alpha-synuclein fibril formation via preferential binding to prefibrillar species. J Biol Chem 280:14733–14740

Dixon C, Mathias N, Zweig RM, Davis DA, Gross DS (2005) Alpha-synuclein targets the plasma membrane via the secretory pathway and induces toxicity in yeast. Genetics 170:47–59

Ellgaard L, Ruddock LW (2005) The human protein disulphide isomerase family: substrate interactions and functional properties. EMBO Rep 6:28–32

Feany MB, Bender WW (2000) A Drosophila model of Parkinson's disease. Nature 404:394–398

Gitler AD, Bevis BJ, Shorter J, Strathearn KE, Hamamichi S, Su LJ, Caldwell KA, Caldwell GA, Rochet JC, McCaffery JM et al (2008) The Parkinson's disease protein alpha-synuclein disrupts cellular Rab homeostasis. Proc Natl Acad Sci USA 105:145–150

Gruber CW, Cemazar M, Heras B, Martin JL, Craik DJ (2006) Protein disulfide isomerase: the structure of oxidative folding. Trends Biochem Sci 31:455–464

Huang C, Ren G, Zhou H, Wang CC (2005) A new method for purification of recombinant human alpha-synuclein in Escherichia coli. Protein Expr Purif 42:173–177

Huang C, Cheng H, Hao S, Zhou H, Zhang X, Gao J, Sun QH, Hu H, Wang CC (2006) Heat shock protein 70 inhibits alpha-synuclein fibril formation via interactions with diverse intermediates. J Mol Biol 364:323–336

Kirik D, Annett LE, Burger C, Muzyczka N, Mandel RJ, Bjorklund A (2003) Nigrostriatal alpha-synucleinopathy induced by viral vector-mediated overexpression of human alpha-synuclein: a new primate model of Parkinson's disease. Proc Natl Acad Sci USA 100:2884–2889

Klappa P, Ruddock LW, Darby NJ, Freedman RB (1998) The b' domain provides the principal peptide-binding site of protein disulfide isomerase but all domains contribute to binding of misfolded proteins. EMBO J 17:927–935

Kontopoulos E, Parvin JD, Feany MB (2006) Alpha-synuclein acts in the nucleus to inhibit histone acetylation and promote neurotoxicity. Hum Mol Genet 15:3012–3023

Kruger R, Kuhn W, Muller T, Woitalla D, Graeber M, Kosel S, Przuntek H, Epplen JT, Schols L, Riess O (1998) Ala30Pro mutation in the gene encoding alpha-synuclein in Parkinson's disease. Nat Genet 18:106–108

Lee HJ, Patel S, Lee SJ (2005) Intravesicular localization and exocytosis of alpha-synuclein and its aggregates. J Neurosci 25:6016–6024

Masliah E, Rockenstein E, Veinbergs I, Mallory M, Hashimoto M, Takeda A, Sagara Y, Sisk A, Mucke L (2000) Dopaminergic loss and inclusion body formation in alpha-synuclein mice: implications for neurodegenerative disorders. Science 287:1265–1269

Munoz E, Oliva R, Obach V, Marti MJ, Pastor P, Ballesta F, Tolosa E (1997) Identification of Spanish familial Parkinson's disease and screening for the Ala53Thr mutation of the alpha-synuclein gene in early onset patients. Neurosci Lett 235:57–60

Papp E, Nardai G, Soti C, Csermely P (2003) Molecular chaperones, stress proteins and redox homeostasis. BioFactors 17:249–257

Pirneskoski A, Klappa P, Lobell M, Williamson RA, Byrne L, Alanen HI, Salo KE, Kivirikko KI, Freedman RB, Ruddock LW (2004) Molecular characterization of the principal substrate binding site of the ubiquitous folding catalyst protein disulfide isomerase. J Biol Chem 279:10374–10381

Polymeropoulos MH, Lavedan C, Leroy E, Ide SE, Dehejia A, Dutra A, Pike B, Root H, Rubenstein J, Boyer R et al (1997) Mutation in the alpha-synuclein gene identified in families with Parkinson's disease. Science 276:2045–2047

Savistchenko J, Krzewska J, Fay N, Melki R (2008) Molecular chaperones and the assembly of the prion Ure2p in vitro. J Biol Chem 283:15732–15739

Smith WW, Jiang H, Pei Z, Tanaka Y, Morita H, Sawa A, Dawson VL, Dawson TM, Ross CA (2005) Endoplasmic reticulum stress and mitochondrial cell death pathways mediate A53T mutant alpha-synuclein-induced toxicity. Hum Mol Genet 14: 3801–3811

Spillantini MG, Crowther RA, Jakes R, Hasegawa M, Goedert M (1998) alpha-Synuclein in filamentous inclusions of Lewy bodies from Parkinson's disease and dementia with lewy bodies. Proc Natl Acad Sci USA 95:6469–6473

Turano C, Coppari S, Altieri F, Ferraro A (2002) Proteins of the PDI family: unpredicted non-ER locations and functions. J Cell Physiol 193:154–163

Uehara T, Nakamura T, Yao D, Shi ZQ, Gu Z, Ma Y, Masliah E, Nomura Y, Lipton SA (2006) S-nitrosylated protein-disulphide isomerase links protein misfolding to neurodegeneration. Nature 441:513–517

Velazquez-Campoy A, Leavitt SA, Freire E (2004) Characterization of protein-protein interactions by isothermal titration calorimetry. Methods Mol Biol 261:35–54

Volles MJ, Lee SJ, Rochet JC, Shtilerman MD, Ding TT, Kessler JC, Lansbury PT Jr (2001) Vesicle permeabilization by protofibrillar alpha-synuclein: implications for the pathogenesis and treatment of Parkinson's disease. Biochemistry 40:7812–7819

Wang HQ, Takahashi R (2007) Expanding insights on the involvement of endoplasmic reticulum stress in Parkinson's disease. Antioxid Redox Signal 9:553–561

Wang L, Li SJ, Sidhu A, Zhu L, Liang Y, Freedman RB, Wang CC (2009) Reconstitution of human Ero1-Lalpha/protein-disulfide isomerase oxidative folding pathway in vitro. Position-dependent differences in role between the a and a' domains of protein-disulfide isomerase. J Biol Chem 284:199–206

Yao Y, Zhou Y, Wang C (1997) Both the isomerase and chaperone activities of protein disulfide isomerase are required for the reactivation of reduced and denatured acidic phospholipase A2. EMBO J 16:651–658

Zarranz JJ, Alegre J, Gomez-Esteban JC, Lezcano E, Ros R, Ampuero I, Vidal L, Hoenicka J, Rodriguez O, Atares B et al (2004) The new mutation, E46K, of alpha-synuclein causes Parkinson and Lewy body dementia. Ann Neurol 55:164–173

Zhang L, Zhang C, Zhu Y, Cai Q, Chan P, Ueda K, Yu S, Yang H (2008) Semi-quantitative analysis of alpha-synuclein in subcellular pools of rat brain neurons: an immunogold electron microscopic study using a C-terminal specific monoclonal antibody. Brain Res 1244:40–52